CYCLIC TESTS RESEARCH ON SEISMIC PERFORMANCE OF PRECAST CONCRETE SEGMENTAL BRIDGE PIERS

Wei Hong yi[1], Ge Ji ping[2] and Wang Zhi qiang[3]

[1] *Professor, Dept. of Bridge Engineering , Tongji University, Shanghai, China*
[2] *PHD Student, Dept. of Bridge Engineering , Tongji University, Shanghai, China*
[3] *Associate Professor, Dept. of Bridge Engineering , Tongji University, Shanghai, China*
Email: bridgejiping@126.com

ABSTRACT :

In the paper, the seismic performance of segmental bridge column with dry joints is investigated through a series of quasi-static tests. The effect of construction type, the existing of additional energy-dissipating device, and the bond condition are selected as the experimental variables. From the experiment, the strength, energy dissipation capacity, residual displacement, general hysteretic behavior and mechanical behavior were obtained. The segmental columns experience opening-closing between the segmental interface under cyclic loading, has no plastic hinge mechanism at the bottom of the column commonly seen in conventional columns. Thus, the similar functionality while less damage to the system is achieved. The residual displacement of segmental bridge column with bonded or unbonded prestressing tendons is less The addition of energy dissipation bars crossing the joint could delay the gap opening, increase the strength and the hysteretic energy dissipation of the column.

KEYWORDS: unbonded and bonded strands, dry joints, segmental bridge columns, cyclic loading.

1. RESEARCH BACKGROUND

The use of precast segmental construction technology for rapid construction in bridge columns has recently gained popularity in the worldwide. The lack of knowledge of seismic performance of a bridge with segmental columns is one of the important reasons which limit the use of such kind of system in China (Zhi-Qiang Wang and Ji-Ping Ge, 2006). Recently, some researches on seismic performance of precast segmental columns have been carried out worldwide (Mander and Cheng, 1997; Hewes and Priestley, 2002; Bilington and Yoon, 2004; Chung-chen chou and Yu-Chih Chen, 2006; et al.). In the other way, residual displacement has been shown to be an important parameter in determining the post-earthquake ability of bridges to sustain aftershocks. The idea of using vertical unbonded prestressing tendons in columns to mitigate residual displacements has been in existence for several years (Zatar and Mutsuyoshi, 2000; Mahin and Sakai, 2006; et al.).

Although a great deal of effort has been made on the research on segmental bridge columns, the behavior under earthquakes is still lacking. The focus of this study is the static cyclic loading and the shaking table test of segmental bridge columns. In this paper the seismic performance of segmental bridge columns under cyclic loading test is investigated, and the results of shaking table test will be presented later.

2. SPECIMEN DESIGN

The test includes four single-column bents specimens, a conventional reinforced concrete bridge column (RC), a precast segmental unbonded prestressing reinforced concrete bridge column (UBPC-S), a precast segmental unbonded prestressing reinforced concrete bridge column with energy-dissipating rebars (UBPC-SD), a precast segmental bonded prestressing reinforced concrete bridge column (BPC-S). The construction type (RC and

UBPC-S), the existing of additional energy-dissipating(ED) device (UBPC-S and UBPC-SD), and the bond condition (UBPC-S and BPC-S) are of the prime research interest in the program. Table 1 shows main characteristics of the test specimens and Figure 1 shows their configurations. Table 2 shows stressing of prestressing tendons. Specimen UBPC-S, UBPC-SD and BPC-S mainly consist of one solid block for loading, five precast rectangular solid segments, and one solid block for foundation. For specimen UBPC-SD, Grade I D10 is the longitudinal mild steel reinforcement being extended across the segment joints and is referred as energy dissipation bars in the paper. No shear keys exist in the adjacent segments. The specimens are designed to fit the capacity limitations of the testing facilities in the laboratory. All these test specimens are independent columns standing on a footing, and having a solid rectangular area of 180 mm x 240 mm in the cross section. The lateral loading point is 1800 mm high from the top surface of the footing, and the ratio of the lateral loading point to the height of the cross section is 7.5, designed to fall in flexure. All stirrup hooks within the footings and columns are 135° bend plus 6 bar diameters extension. The hoop ratio is designed to be 1.1% up to a point 250 mm high from the footing top surface so as to induce bending failure of the column. The size of the coarse aggregates in concrete is 5~25 mm and the concrete is designed to be C40. All units are cast using ready-mixed concrete. The reinforcing bars with expected yield strength of 335 MPa (HRB335) are used for both longitudinal and hoop reinforcement. The prestressing tendons in UBPC-S, UBPC-SD and BPC-S consist of two 12.7 mm (7D4 mm) diameter low-relaxation steel prestressing strands with expected ultimate strength of 1860 MPa . The design axial stress given by prestressing is 3 MPa and is common to UBPC, UBPC-S, UBPC-SD and BPC-S. The axial load ratio is set at 0.10.
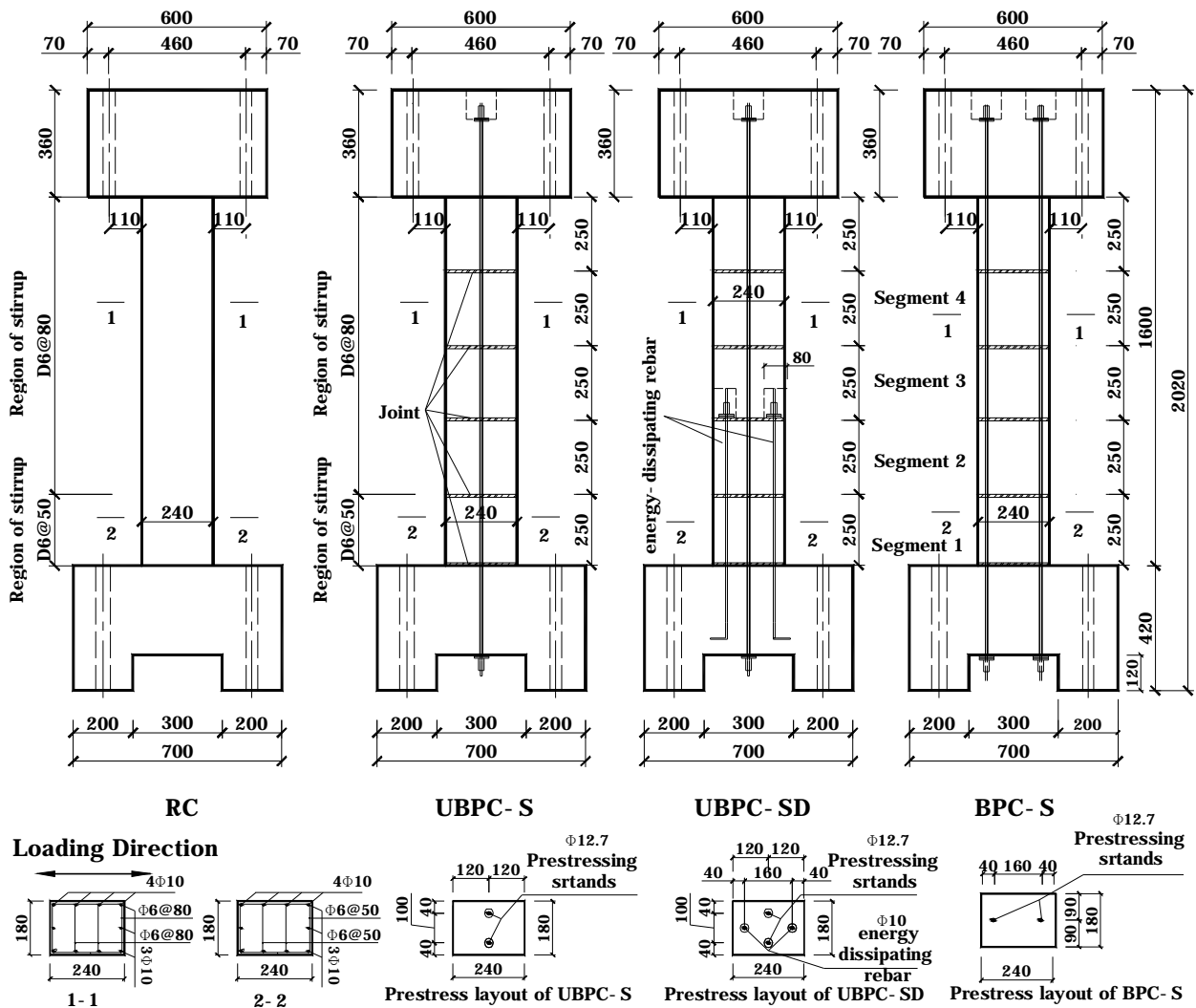
Figure 1 Detail of specimens

Table 1 Characteristics of specimens

Specimen	Longitudinal rebar		Prestressing Tendons		Shear Reinforcement		Construction type	Bond condition
	Rein.	Area ratio(%)	Tendons	Area ratio(%)	Hoops	volumetric ratio(%)		
RC	10D10	1.82%	—	0%	D6@80mm	1.1%	Cast-in-place	—
UBPC-S			2×7D4	0.44%			Precast segment	unbonded
UBPC-SD								
BPC-S								bonded

The following section presents the material properties for concrete and steel used for the test specimens. The average strength of concrete based on three tests on unconfined concrete prismatic block(100×100×300mm), casted during the pour, is measured as 43.2 MPa at 28 days. The concrete compressive strength of expansive concrete mix for pressure grouted to bond the prestressing strands with concrete is 64.1 MPa at 28 days. Table 3 shows the mechanical properties of steel materials. The tensile strength of PC strands is only 80% of expected ultimate strength of PC strands. The reason is that the failure is occurred at the archorage ends, instead of failure away from that. So the tensile strength measured in the paper is not the material strength, but the archorage strength in the specimen. The elastic modulus of concrete, rebar and PC strands is assumed to be 3.45×10^4 MPa, 2.0×10^5 MPa, and 1.95×10^5 MPa separately.

Table 2 Design parameter of stressing

Dead load			Prestressing force			s_{eff} (MPa)	ΔL_{eff} (mm)	ΔL_{max} (mm)
s_c (MPa)	a	P (kN)	s_c (MPa)	a	P (kN)			
2.68	10%	116	3	11.2	65	659	6.1	13

Notes: s_c, the axial stress in the concrete; a, Axial load ratio; P, the magnitude of force; s_{eff}, Prestressing stress after loss; L_{eff}, Prestressing elongation after loss; ΔL_{max}, Maximum allowable elongation

Table 3 Mechanical properties of steel reinforcement and PC strands

Type	Rebar			PC strands
	d=6mm	Grade II d=10mm	Grade I d=10mm	7D5 mm
Yield strength（MPa）	470	350	340	N/A
Tensile strength（MPa）	540	490	500	1500
Extending ratio（%）	25	35	33	N/A

3. LOADING SETUP AND LOADING PROCEDURE

Figure 2 shows the front view of the specimen with the loading apparatus. Curvature was measured at the hinge region. Considering the weight of the superstructure, axial compressive stress applied onto the column head by the actuator was determined to be 2.68 MPa, which was common to all specimens. Then, lateral reversed cyclic displacements were applied with pre-defined cyclic loading protocol, consisting of three drift cycles with amplitudes of 2, 3, 5, 7, 10 mm, followed by three drift cycles with incremental amplitude 5 mm, as shown in Figure 3. Lateral load was applied via a MTS 2000 kN, ±250 mm long-stroke, servo-controlled hydraulic actuator controlled by MTS Flextest digital controller. Reversed cyclic loading ended when the load carrying capacity went below 50% of the observed peak load.
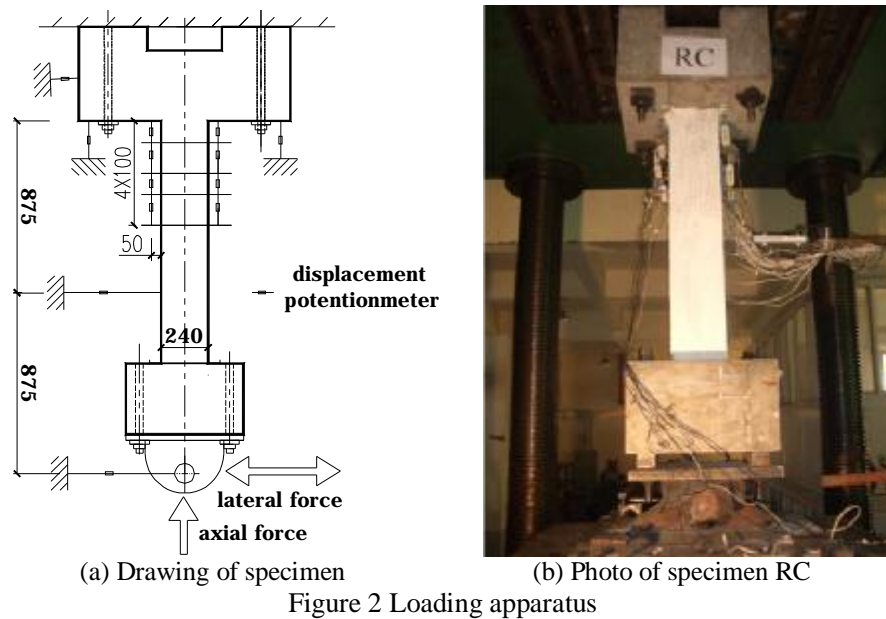
(a) Drawing of specimen   (b) Photo of specimen RC
Figure 2 Loading apparatus
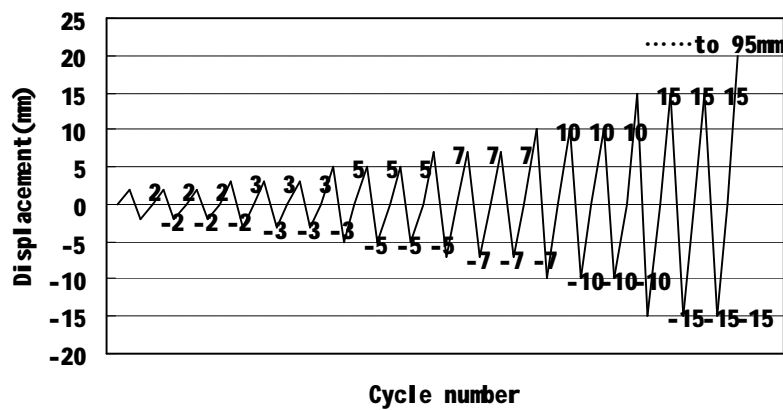
Figure 3 Lateral displacement imposed by MTS actuator

4. TEST RESULTS AND DISCUSSION

4.1 Observed Behavior and Failure Modes

Figure 4 shows the photo of the four specimens at the end of the test. Detailed descriptions of each test can be found elsewhere. General observations about each specimen are described in the following. The damage is more and the location of damage is concentrated in the bottom of the column for specimen RC. For specimen RC, before the maximum compression force was reached, there had been some minor cracks, which was flexural cracks perpendicular to the column axis developed in region closed to the bottom of the columns. Right after the maximum compression force, crack increased with increasing displacements. Then, serious crack increased suddenly and concrete closed to the bottom of the specimen crushed. Finally, confining stirrup expanded outward and reinforcing bars buckled locally. Specimen UBPC-S, UBPC-SD and BPC-S exhibited similar pattern of damage. The amount of damage was less and concentrated in the compression edge of segments for the segmental columns. The gap opening at the joint between segment 1 and the foundation was found to be much larger than those at other joints, limited cracking were found on the surface of segments. The maximum gap openings at the bottom joints were all about 10mm. Due to the use of ED bars, specimen UBPC-SD bent in a way that the gap openings didn't concentrate at the base segment joint comparing to the specimen UBPC-S.

| (a) RC | (b) UBPC-S | (c) UBPC-SD | (d) BPC-S |
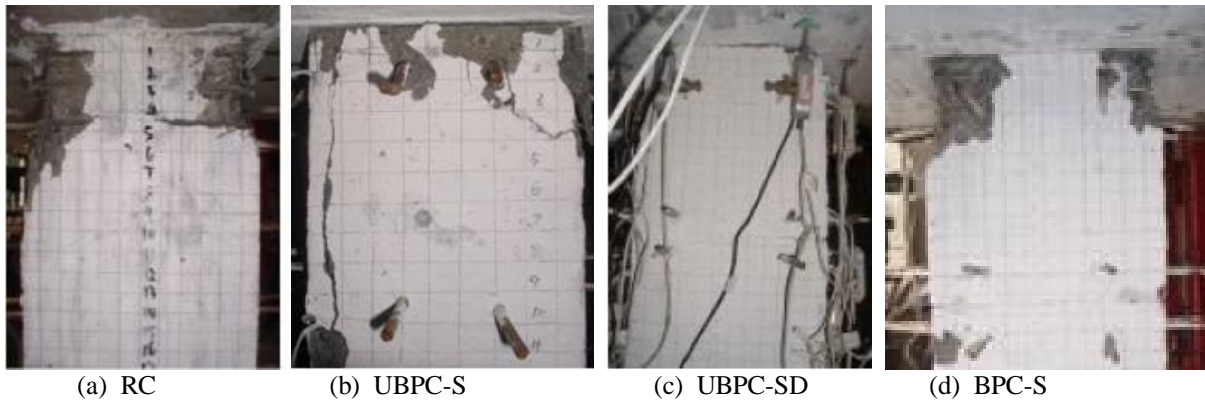
Figure 4 Damage state in the hinge region

(a) RC

(b)UBPC-S

(c)UBPC-SD

(d)BPC-S
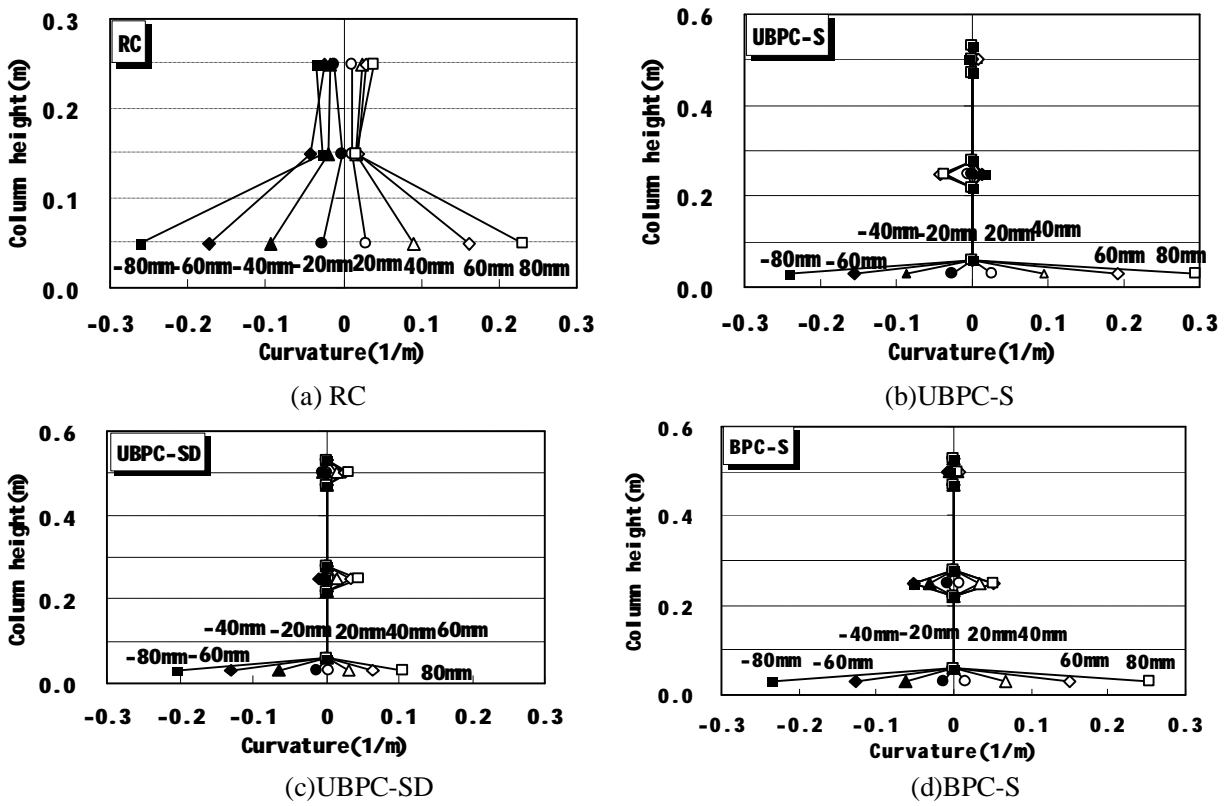
Figure 5 Curvatures along column height

Figure 5 shows the distribution of curvature along the column height for both the push and pull directions. The experimental curvatures were calculated as

$$f = \frac{\Delta_t - \Delta_c}{DL}$$

where Δ_t is the elongation of a displacement transducer on the tension side, Δ_c is the shortening of a displacement transducer on the compression side at the same height level, D is the distance between these two displacement transducers, and L is the gauge length. The gap opening at the base is bigger than that at the interface between other segments, leading to the curvature at the base larger than that at the interface of other segments for all drift levels. The profiles look similar to UBPC-S, UBPC-SD and BPC-S, with curvature concentrated at the base.and at the interface between column segment 1 and 2. Additional lateral restraining to segment 1 and segment 2 of Specimen UBPC-SD, provided by the energy-dissipating bars, reduces rotation of

segment 1. Thus, the curvature of Specimen UBPC-SD (see Figure 5 (c)) at the base is smaller than that of Specimen UBPC-S for all drift.

4.2 Foece-Displacement Relationship Curve

From the displacement versus force curve in Figure 6, it is seen that the hysteretic loops of RC is larger, exhibiting significant hysteretic energy absorption, and the hysteretic loops of UBPC-S and BPC-S is more pinched. Due to the use of ED bars, the strength and the hysteretic energy dissipation of the column UBPC-SD is greatly increased.

(a) RC

(b) UBPC-S

(c) UBPC-SD

(d) BPC-S
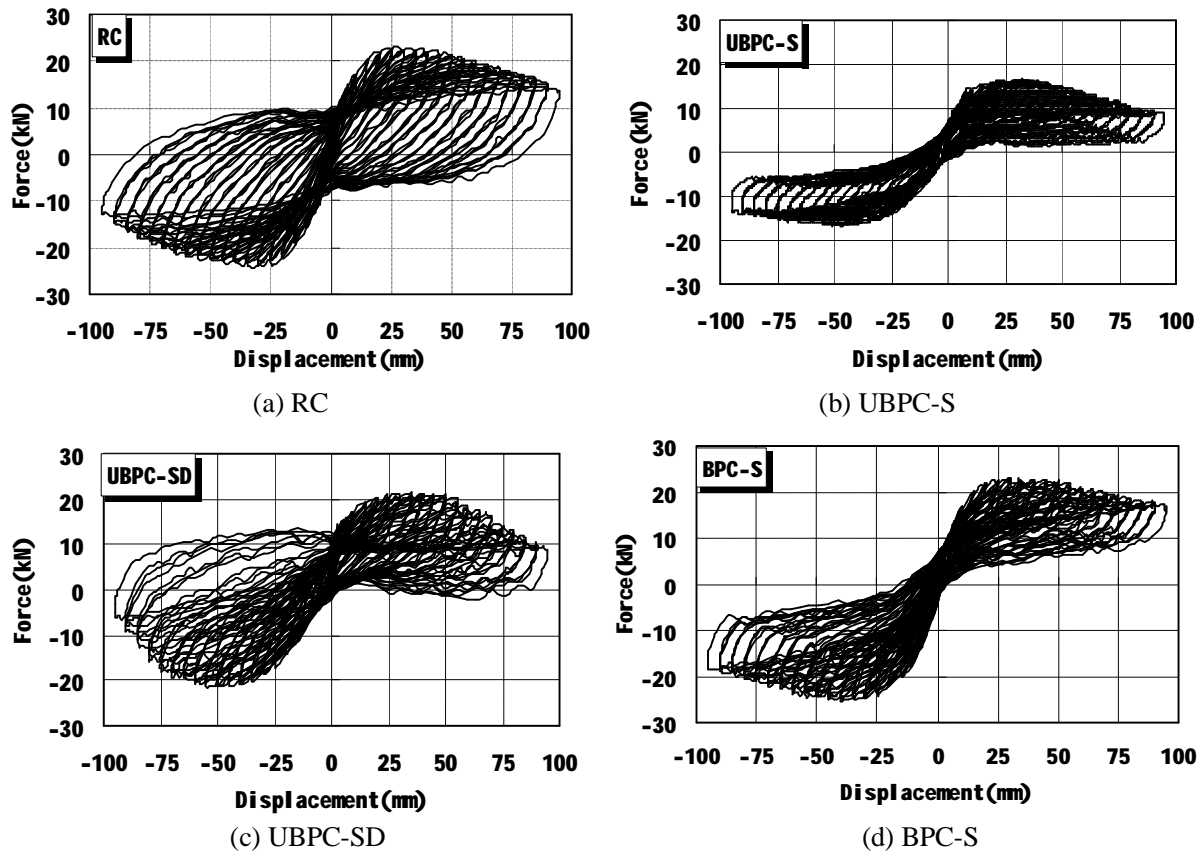
Figure 6 Hysteretic loops of specimens

Table 4 illustrates the strength, top lateral displacements and ductility index, μ. The ductility factor is defined as the displacement at 85% of maximum horizontal force in the decending portion divided by the displacement at the idealized yield point. The yield displacement is defined in Figure 7, according to the area of OTAO equal to that of AKCBA.
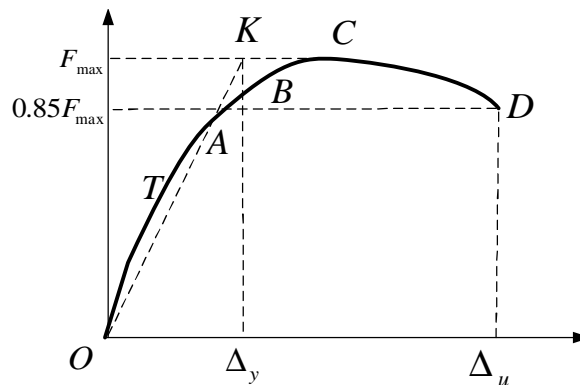
Figure 7 Definition of the yielding displacement and the ultimate displacement

Table 4 .Test results for strength and deformation capacity

Specimen	At first cracking		At idealized yield point		Maximum force F_{max}(kN)	Ultimate force $0.85F_{max}$ (kN)	Maximum Displace-ment Δu(mm)	Ductility index μ
	F_{cr}(kN)	Δ_{cr}(mm)	F_y(kN)	Δ_y(mm)				
RC	20.4	15	23.0	13.8	23.0	19.6	63.5	4.6
UBPC-S	13.1	15	16.3	15.7	16.3	13.9	57.5	3.7
UBPC-SD	15.1	15	21.4	20.3	21.4	18.2	61.7	3.0
BPC-S	20.1	15	22.8	13.8	22.8	19.4	71.2	5.2

Skeleton curve can be acquired by connecting all the peak point of every hysteretic curve with smooth curve. The half skeleton curve marked with labels is shown in Figure 8. The meaning of the labels in Figure 8(a) is referred to Table 5. The meaning of the labels in Figure 8(b) (c) (d) is referred to Table 6.

Bridge columns are expected to undergo large inelastic deformations during severe earthquakes, which can result in permanent or residual displacement. These residual displacements are important measure of post-earthquake functionality in bridges, and can determine whether or not a bridge remain usable following an earthquake. Figure 9 shows a comparison of the relationship between lateral displacement and residual displacement among all specimens. The residual displacement is defined as the displacement of zero-crossing at unloading on the hysteresis loop from the maximum displacement. The specimen RC and UBPC-SD displayed significant residual displacements. These displacements were equal to the peak displacement, meaning small elastic recovery. In contrast, the specimen UBPC-S and BPC-S showed essentially no residual displacements.

Table 5 The meaning of the labels in Figure 8(a)

	A	B	C	D	E
RC	onset of hairline cracks	Maximum bar tensile strain reached 1750 *me*	crushing of concrete cover	Stirrup display	Buckling of rebars

Table 6 The meaning of the labels in Figure 8(b)(c)(d)

state	UBPC-S	UBPC-SD	BPC-S
Gap opening of segment 1 and foundation	A	A	A
Gap opening of segment 1 and 2	B	B	B
Yielding of ED bars		C	
Cover concrete spalling of segment 1	C	D	C
Gap opening of segment 2 and 3		E	
Gap opening of segment 3 and 4		F	
Cover concrete spalling of segment 2	D	G	D
Cover concrete spalling of segment 3		H	
Stirrup display of segment 1	E		E
Stirrup display of segment 3		I	

(a) RC
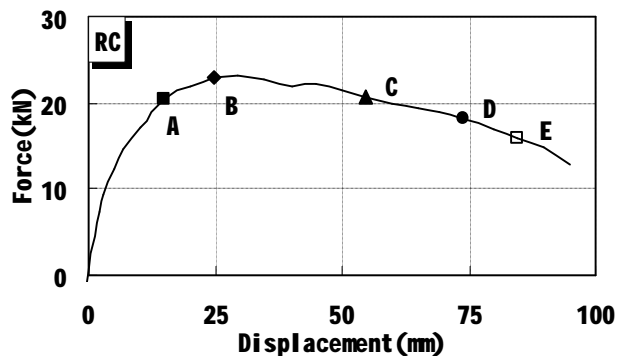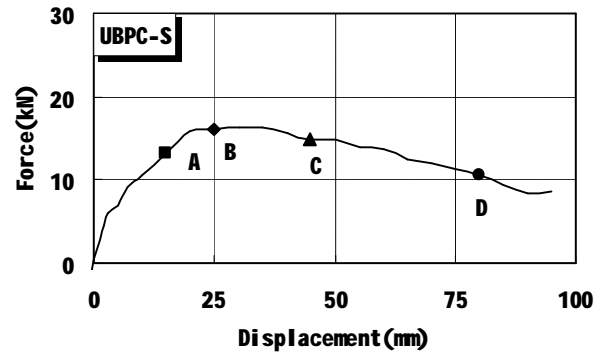
(b) UBPC-S

(c)   UBPC-SD   (d)   BPC-S
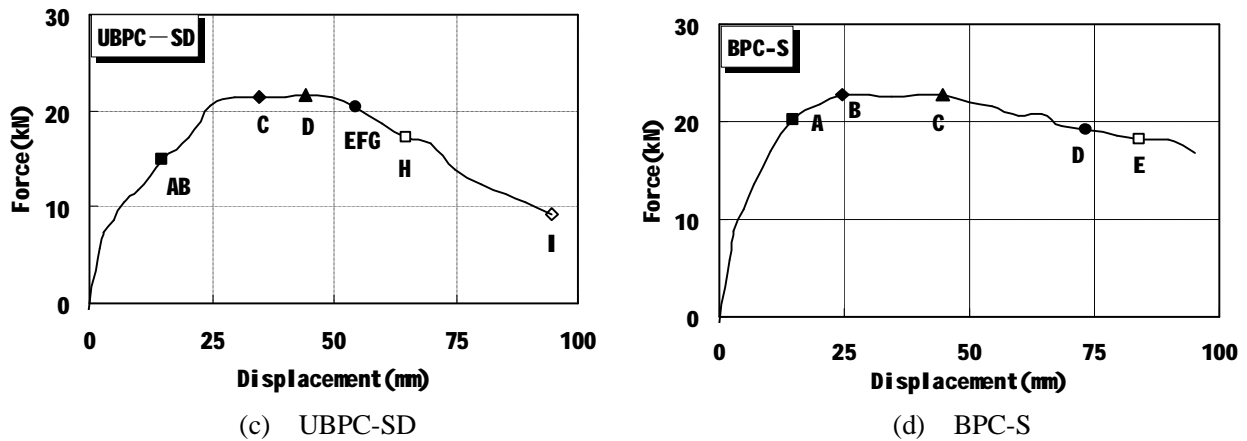
Figure 8 Skeleton curve of specimens
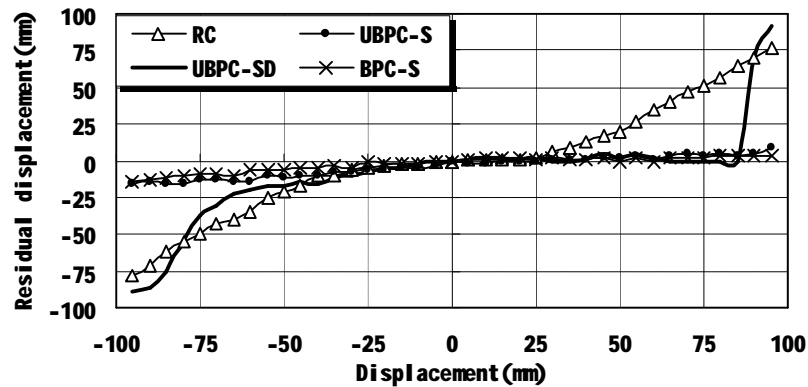
Figure 9 Comparison of residual displacement

5. CONCLUSION

Through the experimental studies of the four specimens having the features of rectangular solid section, construction type, the existing of additional energy-dissipating device, and the bond condition, some important findings are summarized as follows:

1. Although a significant amount of gap opening was observed at critical joint at the end of the test for the segmental columns, the shear still could be successfully transferred across the segmental joints without using shear keys or epoxies.

2. The segmental column experience opening-closing between the segmental interface under cyclic loading, has no plastic hinge mechanism at the bottom of the column commonly seen in conventional columns. Thus, the similar functionality while less damage to the system is achieved.

3. The addition of energy dissipation bars crossing the joint could delay the gap opening, increase the strength and the hysteretic energy dissipation of the column, which will certainly help resist the earthquake.

4. The specimen RC and UBPC-SD displayed significant residual displacements, which equal to the peak displacement, meaning small elastic recovery. In contrast, the specimen UBPC-S and BPC-S showed essentially no residual displacements. Significant seismic performance of segmental bridge column with bonded or unbonded prestressing tendons is achieved.

REFERENCES

Zhi-Qiang Wang and Ji-Ping Ge. (2006). A review of seismic performance study of precast concrete segmental bridge piers. The 9th International Symposium on Structural Engineering for Young Experts in Fuzhou & Xiamen, China:2083-2089.

Mander J.B., and Cheng C.T. (1997). Seismic resistance of bridge piers based on damage avoidance design. Technical Rep. NCEER-97-0014, National Center for Earthquake Engineering Research, Buffalo, State University of New York.

Hewes J.T. (2002). Seismic design and performance of precast concrete segmental bridge columns. PhD Dissertation, San Diego, University of California.

Billington S.L. and Yoon J.K. (2004) . Cyclic response of unbonded posttensioned precast columns with ductile fiber-reinforced concrete. *Journal of Bridge Engineering, ASCE,* **9:4**, 353-363.

Chung-Che Chou and Yu-Chih Chen.(2006). Cyclic tests of post-tensioned precast CFT segmental bridgecolumns with unbonded strands. *Earthquake engineering and structure dynamics*, **35**,159-175.

Zatar W.A., and Mutsuyoshi H. (2000). Reduced residual displacements of partially prestressed concrete bridge piers. 12th World Conference on Earthquake Engineering, Auckland, No. 1111.

Stephen A. Mahin and Junichi Sakai.(2006).Use of Partially Prestressed Reinforced Concrete Columns to Reduce Post-Earthquake Residual Displacements of Bridges. Fifth National Seismic Conference on Bridges & Highways, San Francisco, CA, September 18-20, Paper No. B25.